Chemistry & Biology, Vol. 11, 1279–1291, September, 2004, ©2004 Elsevier Ltd. All rights reserved. DOI 10.1016/j.chembiol.2004.07.012

Modular Synthesis and Preliminary Biological Evaluation of Stereochemically Diverse 1,3-Dioxanes

Jason C. Wong,[1] Scott M. Sternson,[1] Joseph B. Louca,[1] Roger Hong,[1] and Stuart L. Schreiber[1,2,3,*]
[1]Department of Chemistry and Chemical Biology
[2]Howard Hughes Medical Institute
Harvard University
12 Oxford Street
Cambridge, Massachusetts 02138
[3]The Broad Institute of Harvard and MIT
320 Charles Street
Cambridge, Massachusetts 02141

Summary

Modular synthesis and substrate stereocontrol were combined to furnish 18,000 diverse 1,3-dioxanes whose distribution in chemical space rivals that of a reference set of over 2,000 bioactive small molecules. Library quality was assessed at key synthetic stages, culminating in a detailed postsynthesis analysis of purity, yield, and structural characterizability, and the resynthesis of library subsets that did not meet quality standards. The importance of this analysis-resynthesis process is highlighted by the discovery of new biological probes through organismal and protein binding assays, and by determination of the building block and stereochemical basis for their bioactivity. This evaluation of a portion of the 1,3-dioxane library suggests that many additional probes for chemical genetics will be identified as the entire library becomes biologically annotated.

Introduction

Small molecules can be used to modulate protein function and thus to understand biological circuitry in a way that is similar to the use of mutations [1, 2]. This chemical genetic approach to research in the life sciences complements traditional genetics by virtue of the fine temporal control and conditionality of perturbations induced by small molecules in contrast to genetic perturbations [3]. These advantages are important for the study of highly dynamic cellular processes such as cytokinesis, cell division, or signal transduction cascades [4, 5].

Historically, the small molecules used most successfully in chemical genetics have been natural products [6–10]. While natural products are enormously diverse, often complex, and have been frequently useful as probes of biological systems, nonnatural molecules attainable through modern synthetic methodology have the potential to complement, and even to improve upon, the diversity and utility of natural products. In order to access this nonnatural chemical diversity efficiently and comprehensively, new approaches to organic synthesis, such as combinatorial chemistry and diversity-oriented synthesis (DOS), have been undertaken in recent years [11].

Given the remarkable ability of biological systems to recognize and to respond differentially to stereoisomeric molecules, the development of pathways furnishing stereochemically diverse molecules is an important goal within diversity-oriented synthesis. We sought to exploit the enormous structural diversity afforded by the 1,3-dioxane motif **1** (Figure 1A) [12] to generate new nonnatural molecules that would be of use for interrogating biology. At the same time, we reasoned that subsequent biological evaluation of such molecules would provide insight into the relative importance of their diversity elements for modulating biological systems. In our previous synthesis of an 1890 member pilot library based upon the 1,3-dioxane core **1**, we demonstrated the compatibility of the 1,3-dioxane pathway with a solid phase split-pool synthetic platform capable of generating sufficient quantities of individual compounds for multiple protein binding and phenotypic assays [12]. In this pilot library, building blocks were displayed on two distinct, primarily racemic skeletons (Figure 1B). The discovery of new biological probes from this library, and their subsequent use to study such processes as nutrient signaling [13] and organismal development [12], validated the 1,3-dioxane pathway as a source of molecular diversity. These initial results motivated us to synthesize a larger library, described herein, that fully exploits the modular 1,3-dioxane synthetic pathway both by incorporating a more comprehensive set of building blocks and by displaying this diversity on 12 stereochemically distinct, enantioenriched classes of compounds. The 1,3-dioxane pathway detailed herein furnished 18,000 enantioenriched compounds ultimately derived from epoxy alcohols using 17 steps of combined split-pool and parallel synthesis, relying upon a combination of binary encoding with mass confirmation [14] and spatial segregation for structural characterization. In contrast, the pilot 1,3-dioxane library generated 1890 compounds derived from two primarily racemic scaffolds through seven synthetic steps, and relied on mass-encoding and spatial segregation for structural characterization [12].

Results and Discussion

Pathway Expansion: Overview of the Pilot and Extended Libraries

In the original 1,3-dioxane pilot pathway (Figure 2A), three solid-supported epoxy alcohols with general structure **12** were opened to 90 different 1,3-diols **13** with 30 different nucleophiles. A portion of these 1,3-diol intermediates (90 1,3-diols) was set aside and the rest reacted with two dimethylacetals to generate, after Fmoc deprotection, 180 amino-1,3-dioxanes **14**. The amines were acylated with ten electrophiles to give 1800 acylated 1,3-dioxanes **15**, which were cleaved from solid support to give 1,3-dioxanes **1**.

*Correspondence: stuart_schreiber@harvard.edu

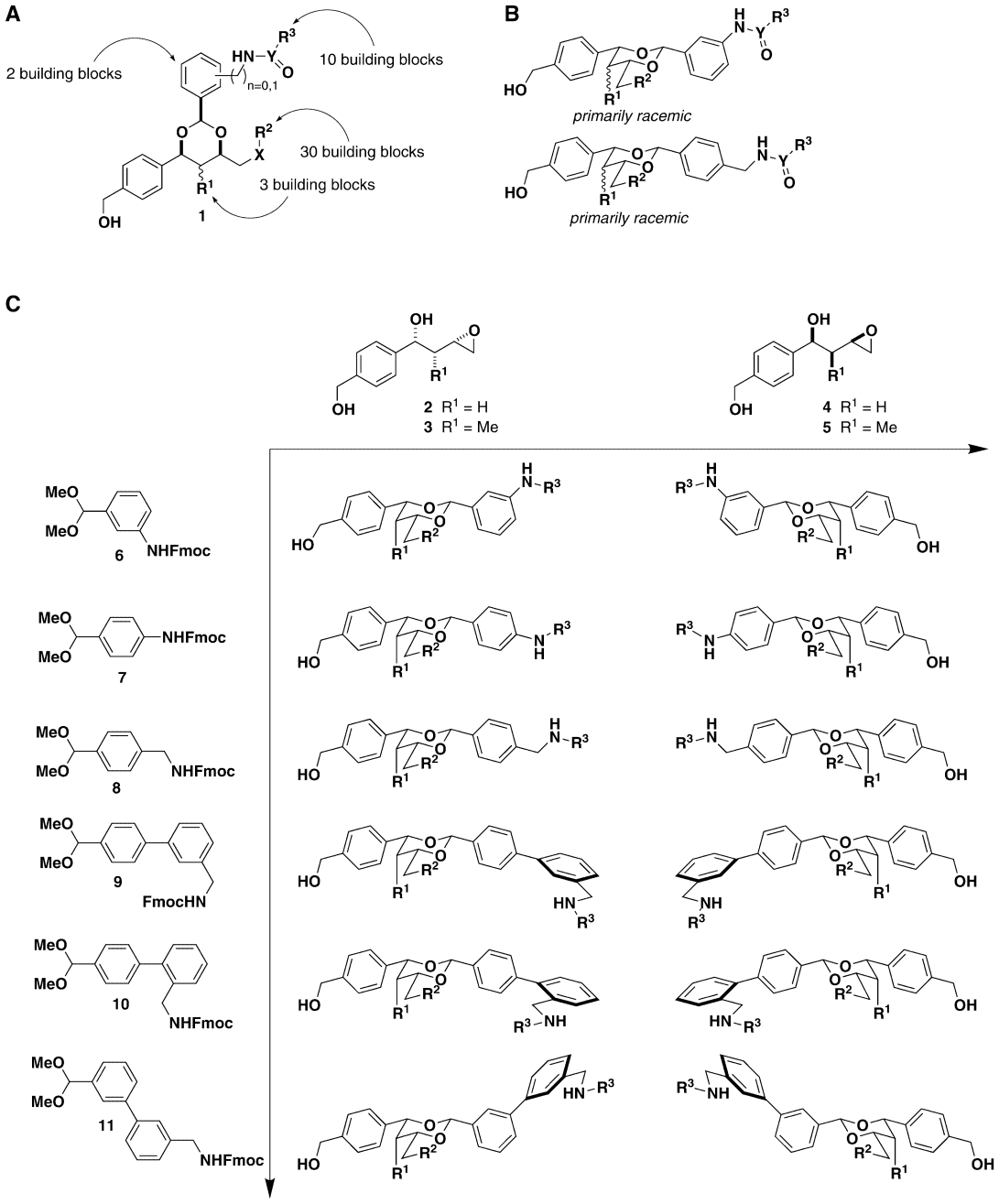

Figure 1. 1,3- Dioxane Pilot Library Overview and Dioxane Stereochemical Diversity

(A) Summary of 1,3-dioxane pilot library with building block incorporation sites.

(B) Two stereochemically diverse scaffolds in the 1,3-dioxane pilot library.

(C) Twelve stereochemically diverse scaffolds in the expanded 1,3-dioxane library.

Besides expanding upon the number and the structural variety of building blocks (detailed below) relative to the pilot synthesis, our extended 1,3-dioxane library pathway also furnished ten new, stereochemically distinct classes of compounds (Figure 1C), 1000 amino-1,3-dioxane intermediates **19**, and included two new reaction classes (Figure 2B). Briefly, four solid-supported enantioenriched epoxy alcohols **16** were opened to 200 different 1,3-diols **17** using 50 thiol and secondary amine nucleophiles. A portion of these 1,3-diols were released from solid support to furnish free 1,3-diols **18** and the rest reacted with six dimethylacetals in a stereocontrolled transketalization to generate, after Fmoc deprotection, 1200 amino-1,3-dioxanes **19**. A portion of these amines was released to give free amines **20,** and the rest reacted with 22 electrophiles to provide 13,200 amides **21**, 1200 sulfonamides **22**, 2400 carboxyamides **23,** 2400 imides **24**, and 7200 ureas **25**.

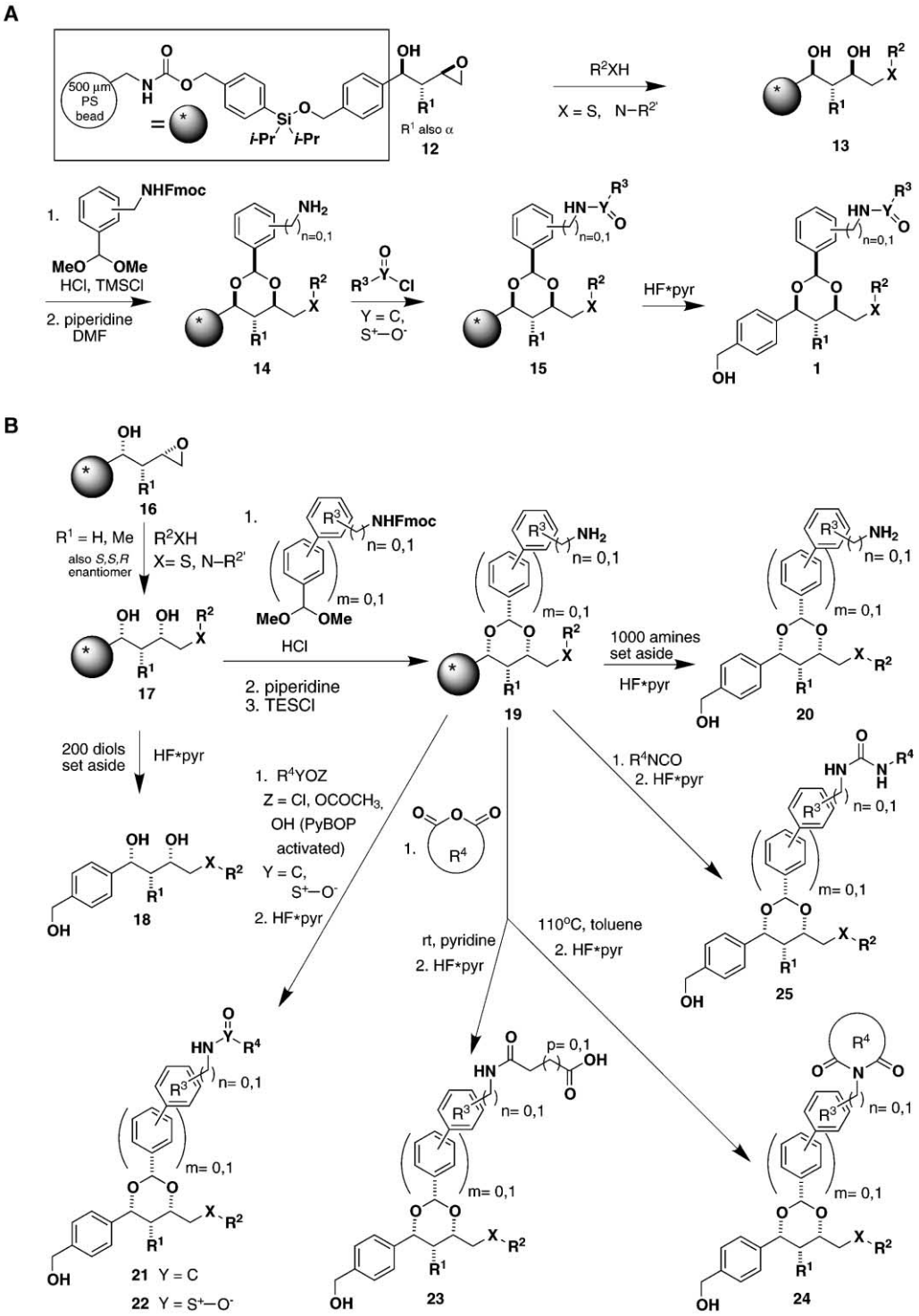

Figure 2. 1,3-Dioxane Synthetic Schemes

(A) Synthetic scheme for the 1,3-dioxane pilot library.

(B) Synthetic scheme for the expanded 1,3-dioxane library.

Nucleophile and Electrophile Building-Block Selection

In addition to 27 nucleophiles from the original pilot library, we selected 23 new nucleophiles containing a variety of acyclic, cyclic nonaromatic, aryl, heteroaromatic, acyclic, and fused polycyclic aromatic motifs for inclusion in our expanded 1,3-dioxane pathway (Figure 3A). We also expanded upon the electrophile diversity of the pilot library by developing conditions for anhydride incorporation, to furnish both carboxyamides and im-

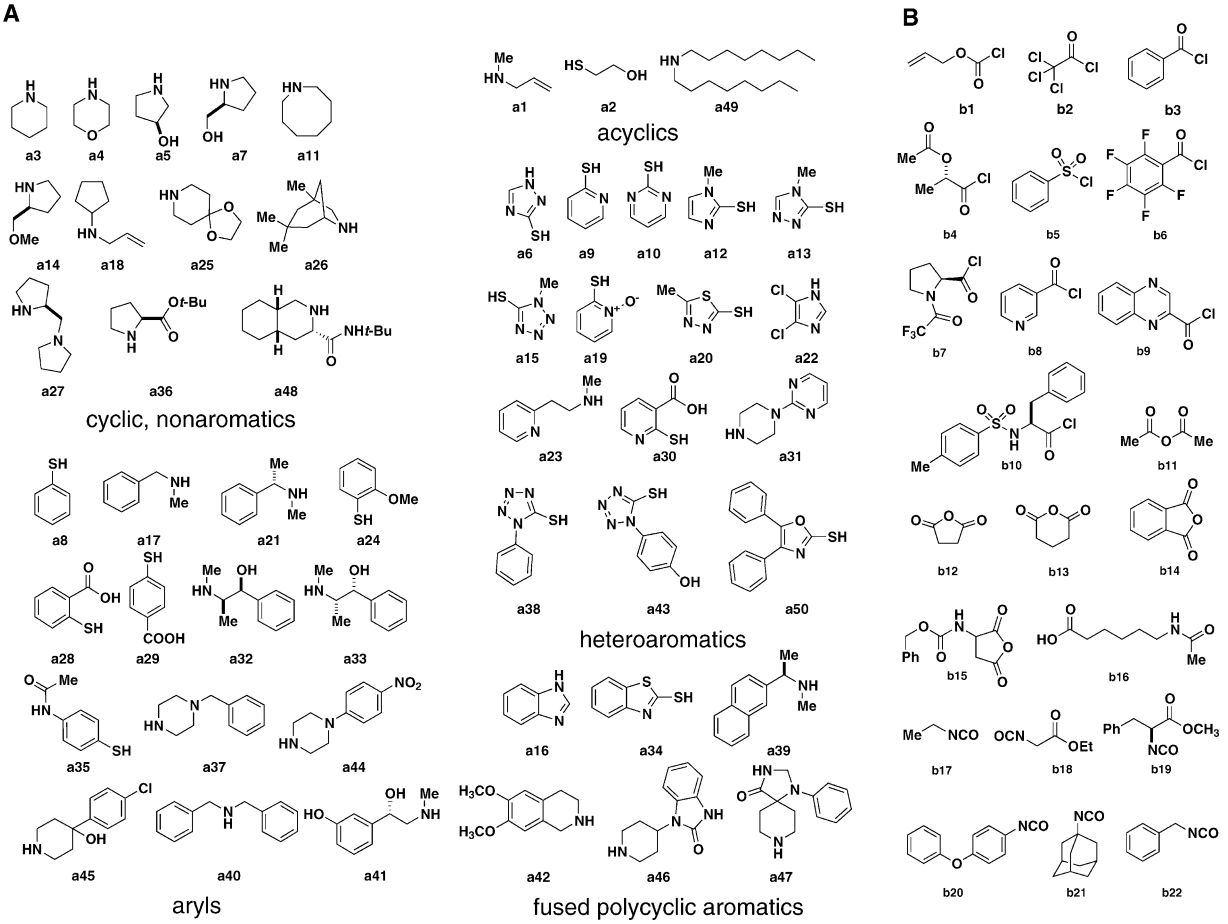

Figure 3. Expanded 1,3-Dioxane Library Building Blocks

(A) Nucleophile building blocks for the expanded 1,3-dioxane library.
(B) Electrophile building blocks for the expanded 1,3-dioxane library.

ides (Figure 3B). Furthermore, we optimized acylation parameters for each electrophile in order to avoid both overacylation and incomplete acylation of amino-1,3-dioxane library intermediates, which significantly affected the purity of the original pilot library (see Experimental Procedures and Supplemental Data). These studies led to the elimination of several electrophiles that consistently generated undesired reaction products (see Supplemental Data).

Library Encoding Strategy

Building block screening studies led to the selection of 50 nucleophiles and 22 electrophiles. Combined in a split-pool approach with the four enantioenriched epoxy alcohols **2–5** and six dimethylacetals **6–11**, these building blocks enabled generation of a $4 \times 50 \times 6 \times 22 = 26{,}400$ member library. Adding to this the 200 diol intermediates **18** and 1,000 amine intermediates **20** generated by the 1,3-dioxane pathway brought the total planned library size to 27,600 members. Because of the size of this library and its high degree of stereochemical and regiochemical diversity, mass redundancy among library members precluded the use of LCMS alone for structural characterization. Instead, each step of the synthetic pathway was encoded by assigning a unique combination of diazoketone tags to each building block (see Supplemental Data), according to the "one-bead one-stock solution" technology platform for chemical genetics [14]. Importantly, to ensure characterization of the library, we assigned the least sensitive tags (tags $T_{10}A$ to $T_{14}A$, which often gave lower intensity signals in GC-ECD detection) to encode for the electrophiles. Because each electrophile had a unique mass, this tagging strategy enabled us to infer electrophile identity by mass spectrometry in cases where the electrophile tag signals were ambiguous.

Library Copy Number

Because of the statistical distributions associated with the split-pool process, ensuring that every member theoretically arising from the pathway is actually generated requires starting with multiple copy numbers of beads. Burgess and coworkers have derived a mathematical relationship between copy number and the percentage of theoretical library members actually synthesized [15]. Using their analysis to approximate the coverage probabilities for the extended 1,3-dioxane library, we determined that a copy number of one would ensure greater

than 65% coverage of library members, while a copy number of three would yield about 95% coverage. Due to the high value of the starting enantioenriched epoxy alcohols and the diminishing returns of screening several-fold greater numbers of mostly redundant compounds, we decided to synthesize a single copy (27,600 beads) of the extended 1,3-dioxane library, or an estimated 18,000 distinct compounds. Two additional copies of the 1,3-diol and amine intermediates were also required to ensure sufficient representation of these molecules in the final library. This called for 2,400 additional beads (400 1,3-diol beads and 2000 amine beads), bringing the total number of beads to 30,000, or 3.6 g of enantioenriched γ,δ-epoxy alcohol functionalized 500–600 μm polystyrene resin **16**.

Library Synthesis

We commenced library synthesis with diazoketone tagging of 900 mg of each of the four γ,δ-epoxy alcohol functionalized resins **16**. After tagging, the resins were pooled, and then split into 50 vessels, tagged for the nucleophile building blocks, and then reacted with 50 different nucleophiles to provide 200 1,3-diols **17**. Approximately 600 of these pooled beads were then set aside for inclusion in the final library as diols **18**. The remainder of the resin was then split and condensed with six dimethylacetals to form 1200 1,3-dioxanes, which were subsequently tagged for the dioxane-forming step. The resin was then briefly washed with PPTS to remove any mixed acetals resulting from the reaction of dimethylacetals with nucleophile hydroxyl groups. At this point, approximately 600 beads from each amine pool (except for the *para*-aniline dioxanes) were set aside for Fmoc cleavage and inclusion in the final library as amines **20**. The remaining 1,3-dioxane resin was pooled and reacted with TESCl to protect nucleophile hydroxyl groups, and then split into 22 vessels. The resin was then tagged before Fmoc cleavage to avoid undesired reaction of the carbenoid tags with free primary amine. After Fmoc cleavage, the amine resin **19** was acylated with 22 electrophiles to yield the final 1,3-dioxane library members **21–25**.

Evaluation of Synthetic Purity, Yield, and Encoding Fidelity throughout the Synthesis

Synthetic Purity

After each building block-incorporating step of the synthesis, and before the next pooling step, we randomly selected a number of beads from different pools for compound and tag cleavage to evaluate both the purity of each synthetic transformation and the fidelity of the encoding procedure.

As shown (Figure 4A), of the 13 diols **18** analyzed by LC, all were greater than 70% pure and 12 out of 13 were greater than 90% pure. Of the ten amines **20** analyzed by LC, nine were greater than 70% pure and eight were greater than 90% pure. Of the 128 acylations **21–25** analyzed by LC, 53% were greater than 90% pure and 76% greater than 70% pure. Acylation of insufficiently protected nucleophile hydroxyl groups accounted for the major impurities in 5% of the reactions less than 90% pure, while incomplete acylation was observed in 7% of the reactions less than 90% pure (Figure 4C). No oxidation (M+16 by mass spectrometry) byproducts were detected.

The purities we observed for the full library pathway were comparable to those of the original 1,3-dioxane pilot library (Figure 4A). In fact, there was a significant reduction in the number of reactions in which overacylation, incomplete acylation, or oxidation was observed as compared to the pilot library (Figure 4C). Our optimization of the acylation step and use of the TESCl hydroxyl-protecting group were thus key factors in improving this aspect of the split-pool synthesis. The relative increase in the percentage of reactions containing other unidentifiable impurities was attributed primarily to the introduction of new acylation reactions and building blocks (see Supplemental Data for purity analysis by acylation reaction class). Nevertheless, the overall purity of the full library exceeded that of the pilot library.

Encoding Fidelity

In addition to evaluating the purity of each reaction of the synthetic pathway, we also analyzed the fidelity of the corresponding tagging process (Figure 4D), which is critical for the identification and resynthesis of molecules, as well as for the correlation of structure with bioactivity. A total of 131 of 151 structures determined by LCMS and pool origin were consistent with structures predicted by GC-ECD tag analysis. Nine additional compounds gave MS data that were reconciled with tag analysis after we considered possible undesired transformations using knowledge of the synthetic pathway. For example, in three cases, the mass we observed was consistent with acylation of an insufficiently protected hydroxyl-containing nucleophile (in addition to acylation at the desired site). After this reaction was taken into account, the observed mass and GC prediction were fully concordant. We were able to infer nine compounds from GC traces alone despite low intensity LC traces, while one compound gave ambiguous tags but was partially identifiable by mass alone. Inconsistency between LCMS and GC data was observed in only one case out of 151 compounds. Our analysis demonstrates that in the vast majority of cases, LCMS data, GC data, and knowledge of the synthetic pathway enable predictions of structure, including stereochemistry and regiochemistry, to be made confidently.

Synthetic Yield

Using Fmoc quantitation, we determined the loading level, or amount of compound, per bead at the amine intermediate stage just prior to generation of **19**. The average loading level was found to be 52 nmol/bead, or 88% of the 59 nmol/bead determined from bulk elution and purification of a model 1,3-dioxane compound (Figure 4B) [12]. We also integrated the LCMS traces of 58 final products and converted peak areas to concentrations using a molar absorptivity value typical of 1,3-dioxane library members, in order to obtain a rough loading level estimate for the final stage of the library synthesis. This analysis furnished a loading level of 20 nmol/bead, or 34% of the model compound loading level (Figure 4B). The discrepancy between this value and the value determined at the amine intermediate stage could have been due to partial compound cleavage during TESCl protection or electrophile acylation. Alternatively,

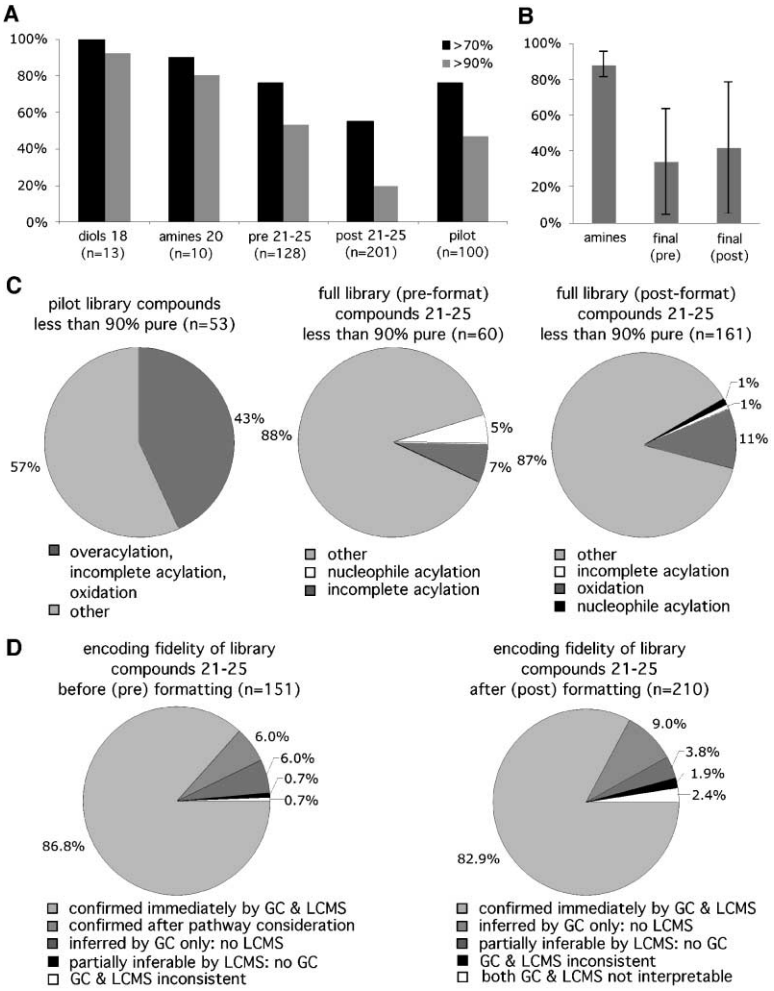

Figure 4. Analysis of Library Purity, Structural Characterization, and Synthetic Yield

(A) Purity analysis of library intermediates and final products before (pre) and after (post) formatting in comparison with pilot library purity. y axis: percent reactions analyzed; n = no. of beads analyzed.

(B) Synthetic yield on a per bead basis at various stages of library synthesis as a percentage of the yield obtained from bulk cleavage of a model compound. Error bars indicate standard deviation.

(C) Analysis of characterizable impurities in reactions less than 90% pure by LCMS from the pilot and expanded libraries (both pre- and postformat). n = no. of beads analyzed.

(D) Analysis of structural characterizability on a per bead basis before (pre) and after (post) library formatting. n = no. of beads analyzed.

this value may not be an accurate measure of the actual loading level due to variation in the molar absorptivity of the 1,3-dioxanes analyzed. Nevertheless, these data allowed us to place a reasonable upper and lower bound on the loading level for the majority of individual beads. Assuming, for example, that the material released from a single bead is dissolved in 10 μl of DMSO, the stock solution thus produced would have a concentration within the range of 2–5 mM. This range is suitable for performing multiple screens (each requiring ~100 nl DMSO solution) with final compound concentrations at the low micromolar level. Combined with purity analysis, these results thus demonstrated the overall synthetic efficiency and yield of the 1,3-dioxane pathway on a per bead basis, ensuring that the majority of beads contain sufficient quantity and purity of compound for multiple biological assays [12, 16].

Library Formatting

After we evaluated the purity, encoding fidelity, and yield of the extended 1,3-dioxane pathway, individual beads were formatted into 384-well plates for compound release and biological evaluation. Acylated dioxane resins **21–25** (about 26,400 beads) were arrayed into 73 384-well plates, amine intermediate resin **20** (about 3000 beads, 3 copies) into 9 384-well plates, and diol intermediate resin **18** (600 beads, 3 copies) into 2 384-well plates. Compounds were then robotically cleaved and formatted into stock solutions for phenotypic and protein binding assays as previously described [16]. Prior to biological evaluation, we once again analyzed individual formatted compounds for purity, encoding fidelity, and yield.

Evaluation of Synthetic Purity, Yield, and Encoding Fidelity of the Acylated Dioxanes

We selected approximately 1% of the compounds (three wells) from each plate for purity and encoding fidelity analysis. As shown (Figure 4A), 20% percent of the acylated dioxanes **21–25** analyzed were greater than 90% pure and 55% were greater than 70% pure. Of the reactions that were less than 90% pure, 11% contained impurities resulting from sulfide oxidation, 1% contained overacylation products, and 1% contained free amine due to incomplete acylation (Figure 4C). Sulfide oxidation thus accounted for a significant portion of the impurities introduced through the formatting process. It is likely that extensive compound manipulation during this process was responsible for higher levels of air exposure leading to compound degradation.

As shown (Figure 4D), 83% of the acylated dioxanes analyzed gave clear MS signals and came from beads furnishing readily interpretable GC tag traces, enabling unambiguous structural identification and confirmation. Nine percent of the compounds analyzed gave interpretable GC tag traces but very low intensity LCMS traces. This percentage was comparable to the 7% of acylated dioxanes analyzed before formatting that had low LCMS traces (9 out of 128). We attributed the slight increase in compounds with low LCMS traces to degradation during formatting. Approximately 4% of the acylated dioxanes gave ambiguous GC traces, most likely due either to failure of tag incorporation, tag cleavage, or tag derivitization for GC analysis. The remaining 4% either had inconsistent LCMS and GC data, or gave uninterpretable data. In cases where tags were ambiguous, mass data alone was sufficient to propose a small set of possible compounds, which, for the purposes of assay follow up, could be resynthesized and reevaluated if necessary. These results indicated to us that while encoding fidelity was somewhat diminished through the process of formatting 30,000 individual beads, in the majority of cases (>80%) confident structure prediction could still be made.

To determine the average amount of final compound released per bead after the formatting process (not including those beads that gave very low intensity LC traces), we resynthesized ten representative dioxanes identified during purity and encoding fidelity analyses (see Supplemental Data). LC analysis of serial dilutions of these compounds furnished molar absorptivities that we then used to determine the concentrations of the original stock solutions of these compounds in the formatted library (Figure 4B). We found the average loading level to be 24 nmol/bead, which was consistent with the loading level estimate of 20 nmol/bead determined prior to library formatting. These results provide a more comprehensive measure of the synthetic yield of the 1,3-dioxane pathway, in contrast to the loading level analysis performed for the pilot library, where a single representative compound was evaluated [12].

Synthetic Purity, Yield, and Encoding Fidelity of Amines and Diols

While we expected the amine **20** and diol **18** sublibraries to have the highest purity based on analysis prior to library formatting, the purity of these compounds appeared to have been significantly decreased by the formatting process. Weak or complex LC traces from the majority of wells suggested significant compound degradation. Because of the relatively small size of these two sublibraries and their potential value for biological exploration, we decided to adapt this portion of the 1,3-dioxane pathway to a solid-phase parallel synthesis format for rapid resynthesis.

Parallel Synthesis Model Studies

Successful parallel resynthesis of the amines and diols from the 1,3-dioxane pathway depended upon the feasibility of conducting 1000 acid-catalyzed ketalization reactions in a reasonable timeframe and with a limited quantity of starting materials. Adaptation of the 1,3-dioxane-forming reaction to 96-well plate format was therefore crucial to parallel library realization.

Model 1,3-diol substrates **26, 28,** and **33** (Figures 5A and 5B) were subjected to microplate-scale conditions for dioxane formation. Reactions with **28** and **33** proceeded in high purity; however, reactions with **26** in microplate-scale format consistently gave an additional peak in the LC trace, regardless of reaction conditions or dimethylacetal. We identified this side product as chloride **27** (Figure 5A) and postulated that it arose from hydroxyl-assisted chloride displacement of the amine in substrate **26** that competes with dioxane formation. We did not observe this side reaction with **28** as substrate because dioxane formation proceeds more rapidly without methyl substitution at R^1. Presumably, generation of **27** from sulfide **33** was also not observed because the lower basicity of the sulfide would hinder the competing displacment process. In the end, these model studies led us to remove the methyl epoxyol substrates from the resynthesis pathway.

To evaluate the substrate generality of the parallel format ketalization, we combined 1,3-diol substrates **28–33** and dimethylacetals **6–11** (not including **7**) in 96-well plate format (Figure 5B). The high purity of these test reactions (see Supplemental Data) demonstrated compatibility of the 1,3-dioxane pathway with a 96-well format for parallel resynthesis.

Parallel Synthesis of the Amine and Diol Library Subsets

Synthesis of the parallel library (Figure 5C) commenced by opening the two epoxy alcohol enantiomers **34** and **35** with the 50 nucleophiles from the encoded library pathway (with the exception of nucleophile **a26,** which we replaced with the enantiomer of **a7**). Purity analysis of the resulting 1,3-diols **36** led us to eliminate nucleophiles **a31** and **a41**, leaving 96 total substrates for ketalization.

We then prepared five 96-well plates, each containing the 96 1,3-diol substrates (eight identical beads per well) for 1,3-dioxane formation. Each plate was subjected to one of the five dimethylacetals, **6**, **8**, **9**, **10**, or **11**, under sealed, argon-blanketed, acid-catalyzed reaction conditions. After 1,3-dioxane formation to give **37**, 24 wells with free hydroxyl-containing nucleophiles were washed with PPTS to remove mixed acetal impurities. We set aside the remaining 1,3-diol beads **36** for inclusion in the final 576-member sublibrary.

Evaluation of Synthetic Purity and Yield

After completion of the synthesis, we analyzed the diol and amine sublibraries for purity by LCMS (Figure 6A). Of the 19 diols **36** analyzed, 9 were greater than 90% pure and 14 were greater than 70% pure. Of the 131 Fmoc-protected amines **37** analyzed, 70% were greater than 90% pure, 83% greater than 80% pure, and 90% greater than 70% pure; 5% gave no LC trace, while the major impurity in 51% of the reactions less than 90% pure (20 out of 39 reactions) was due to sulfide oxidation (M+16 by mass spectrometry). We attributed the apparent increase in Fmoc-amine purity, as compared with 1,3-diol purity (Figure 6A), to the fluorenyl chromophore,

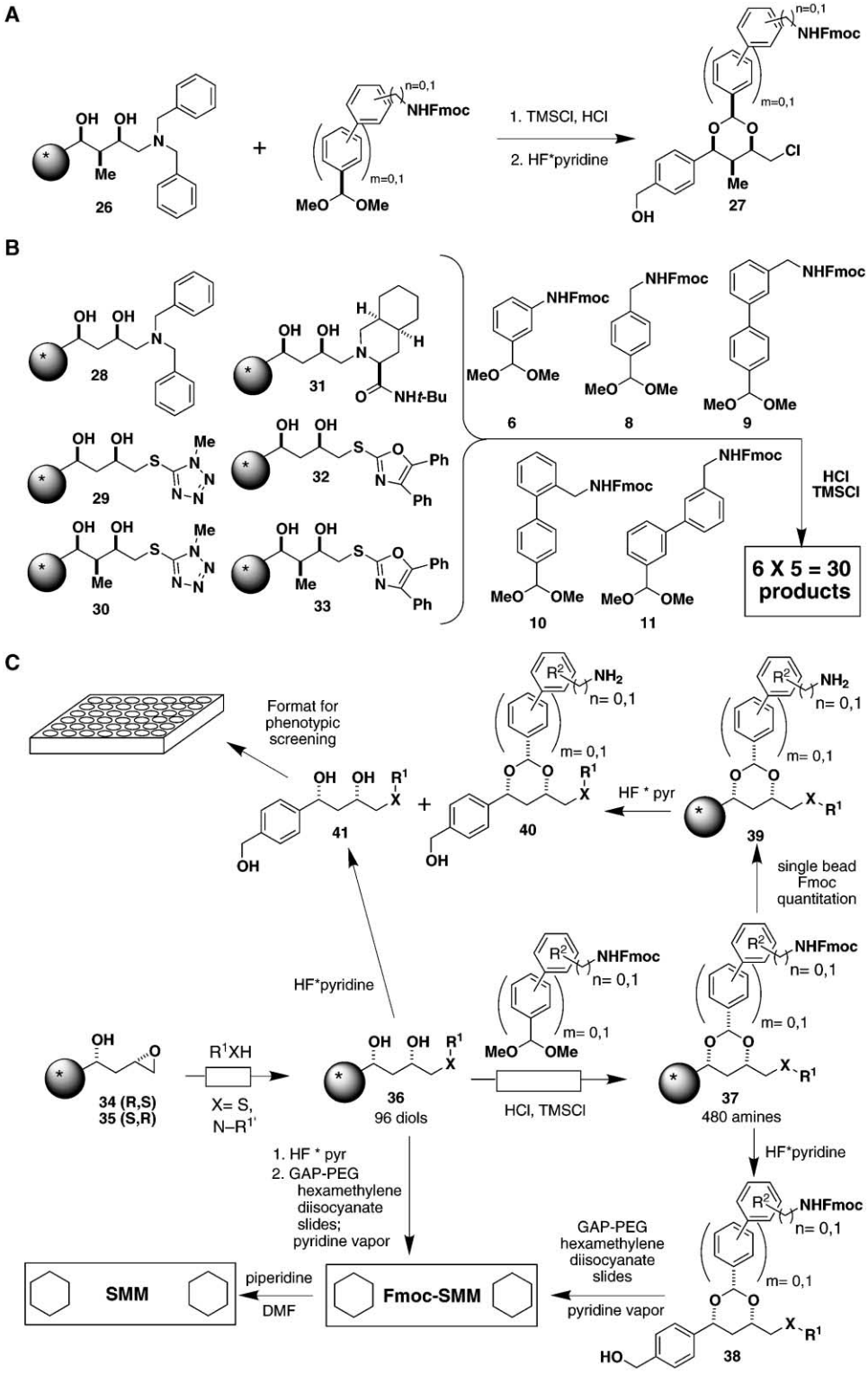

Figure 5. Parallel Synthesis Model Studies and Schemes

(A) Identification of an impurity that arose in microplate synthesis format.

(B) Model compounds used in a test matrix to demonstrate dioxane pathway compatibility with a microplate synthesis format.

(C) Parallel synthesis and formatting scheme. Box arrows indicate parallel synthesis step.

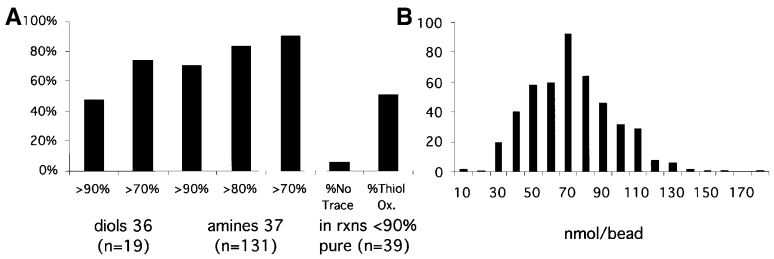

Figure 6. Analysis of Purity and Yield of the Parallel Library Synthesis

(A) Purity analysis of the parallel library, including identifiable impurities. y axis: percent reactions analyzed.

(B) Single bead loading levels as determined by Fmoc quantitation. y axis: number of beads.

which systematically affected the molar absorptivity of these compounds.

We also subjected Fmoc-protected amine beads to single-bead Fmoc-quantitation in 96-well plate format (Figure 6B). The average loading level for the 480 beads analyzed was 67 nmol/bead, comparable to the loading levels previously determined for the extended 1,3-dioxane library at the amine intermediate stage. Ninety-five percent of the single bead loading levels were less than 2-fold lower or greater than the average loading level, ensuring that library formatting would furnish stock solutions with a relatively narrow range of concentrations.

Small-Molecule Microarrays for Protein Binding Assays

The Fmoc-amine **38** and diol subsets **41** were robotically printed [17] onto γ-aminopropyl microscope slides derivitized with a short diethylene glycol spacer using diisocyanate capture chemistry. We spatially arrayed the compounds (see Supplemental Data) such that structural trends in binding could be immediately assessed upon visual inspection of the slide. To demonstrate the success of 1,3-dioxane library synthesis, formatting, and printing, fluorescently labeled calmodulin was incubated with Fmoc-deprotected slides to identify small-molecule calmodulin binders. As shown (Figure 7A), a specific set of spots lighted up above background on the array, corresponding to amines containing the heptamethyleneimine building block **a11**. Importantly, we did not reproducibly detect any other spots above background, suggesting that this structural feature is essential for calmodulin affinity. These initial results were confirmed by resynthesizing representative amino-1,3-dioxane **42** and determining its calmodulin binding constant by surface plasmon resonance.

A Whole Organism Phenotypic Assay

We then screened 96 diols **41** and 288 amino-1,3-dioxanes **40** representative of the 1,3-dioxane pathway in zebrafish developmental assays [18] to identify potential modulators of development or organ function. Briefly, embryos at the 128–256 cell stage were incubated with compound (5–10 μM) in embryo buffer containing 0.1% DMSO over a period of several days. Observations were made at 28 hr postfertilization (hpf), 48 hpf, and 72 hpf. Interesting phenotypes were noted only in those cases where all three embryos in a given well were affected. We found that one amino-1,3-dioxane **43**, but not its enantiomer **44** or related analogs **45**, **46**, and **47** (Figure 7B), specifically induced cardiovascular malfunction in developing zebrafish, which was imaged at 5 days postfertilization (dpf) as shown (Figure 7C). Preliminary dose-response experiments with resynthesized **43** in 2 dpf zebrafish demonstrated that **43** induces reversible 2:1 atrioventricular block [19] at 6 μM within 15 min of treatment (data not shown). This rapid, potent, specific, and reversible effect led us to speculate that **43** may target a cardiomyocyte-specific ion channel important for repolarization [20], such as the zebrafish ortholog of the hERG potassium channel [21]. Developmental perturbation was deemed less likely, as the zebrafish cardiovascular system is fully developed by 2 dpf [19]. Despite the challenges of testing small molecules in whole organisms, the one bead-one stock solution approach enabled identification of a a bioactive molecule using less than 5% of the stock solution derived from a single bead.

1,3-Dioxane Contribution to Nonnatural Molecular Diversity

To assess the molecular diversity generated by our expanded 1,3-dioxane pathway and its contribution to the population of chemical space, we used QSARIS (SciVision) to calculate more than 100 molecular descriptors for representative library members (diols, amines, and acylated 1,3-dioxanes derived from **2**, **6**, and **9**) and known bioactives. The dimensionality of this data set was reduced using principal component analysis [22], providing three principal component axes capturing 35% of the information contained within the 100+ dimensional space. As depicted (Figure 7D), the diversity and distribution of these compounds compares favorably with a set of over 2000 known bioactive compounds. Notably, many of these members are located in previously unpopulated regions of this space. While the bioactive compounds identified herein lie along the periphery of the known bioactive set (Figure 7E), it is possible that as the entire 1,3-dioxane library is evaluated, regions further from the bioactive set will be found to harbor biological activity as well.

Our studies demonstrate that extensive evaluation of purity, efficiency, and encoding fidelity for a representative number of individual library members at each step of library construction is an integral part to the synthesis of large-member libraries suitable for biological evaluation. Careful attention to the metrics of synthetic quality is especially important when pathway chemistry is attempted in the presence of a wide range of functionality and structure. This analysis enables the rational resynthesis of library subsets when necessary and provides concentration, purity, and structural information crucial to obtaining meaningful information from biological screens of the library.

Our preliminary evaluation of the library in chemical

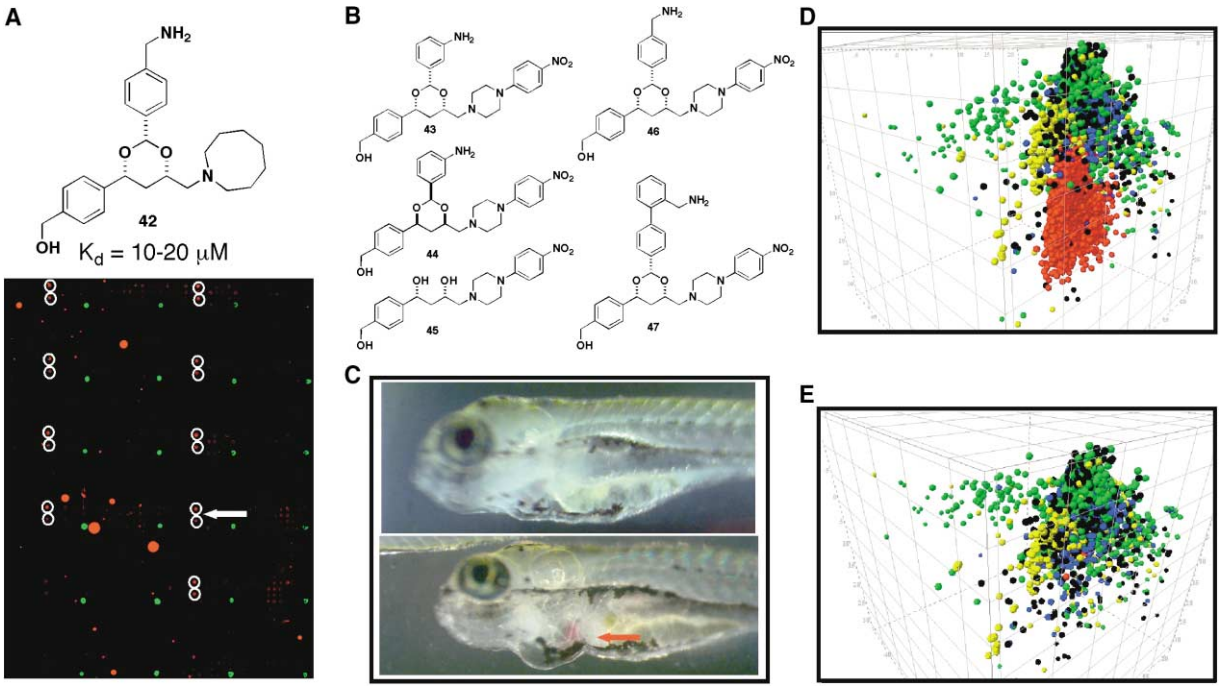

Figure 7. Preliminary Biological Evaluation of the Expanded 1,3-Dioxane Library

(A) Small-molecule microarray of 1,3-dioxane amines and diols screened against Cy5-labeled calmodulin. Circled spots indicate reproducible positives all containing building block a11. Each circled spot falls within the microarray grid and is above background staining levels. Arrow indicates representative compound **42** that was resynthesized and analyzed by surface plasmon resonance to determine its binding constant.

(B) 1,3-dioxane **43** that induced cardiovascular malfunction in 2 dpf zebrafish along with other analogs that were inactive in the zebrafish screen.

(C) Top: control fish after 5 dpf. Bottom: fish treated with **43** (3 μM) after 5 dpf. Arrow indicates erythrocyte buildup and pericardial edema.

(D) 1,3-dioxanes (red) and over 2000 known bioactives (various colors) plotted in molecular diversity space. The distribution and diversity resulting from the 1,3-dioxane pathway rivals that of the bioactive conglomerate.

(E) Known bioactives with two 1,3-dioxanes identified through microarray and zebrafish screens (top red sphere = **a11**-containing 1,3-dioxane derived from dimethylacetal **6**; bottom red sphere = **43**).

genetic screens demonstrates the promising bioactivity of the enantioenriched 1,3-dioxanes and confirms the importance of building block, stereochemical, and skeletal diversity for the discovery of new biological probes. In particular, the modularity of the 1,3-dioxane pathway enabled us to incorporate a large set of diverse nucleophiles, of which one was found to be consistently important for binding to calmodulin. Furthermore, stereocontrolled synthesis of library members through the use of enantioenriched epoxy alcohols allowed individual nucleophiles and electrophiles to explore various three-dimensional orientations, diversity we demonstrated to be crucial for the discovery of an inhibitor of cardiovascular function in zebrafish.

Significance

We have synthesized 18,000 stereochemically and skeletally distinct enantioenriched molecules whose diversity and distribution in chemical space has been compared to that of a set of over 2,000 known bioactive compounds. Extensive analysis of library quality at each stage of the synthesis is detailed and shown to be important in the generation of large-member libraries suitable for biological evaluation. In particular, as efforts to expand the toolbox of available small-molecule probes for chemical genetics increase in frequency and intensity, the ability to map biological assay data to well-characterized molecular libraries will be crucial. Our discovery of a building block-specific calmodulin binding element and an inhibitor of heart function whose bioactivity was not manifested by its enantiomer illustrate the respective contributions of building block and stereochemical diversity to small-molecule-facilitated studies in biology.

Experimental Procedures

General Protocols

General protocols for resin cleavage, encoding and decoding of resins, LCMS analysis of reaction product purity, electrophile screening, and acylation optimization are provided in the Supplemental Data.

Solution Phase Synthesis Procedures

Solution phase preparation of building blocks and epoxy alcohol loading onto solid support have been described previously [23] with the exception of the synthesis of methyl epoxy alcohols, for which a representative procedure is available (see Supplemental Data).

Library Synthesis

1,3-Diol Resin (17)

γ,δ-epoxy alcohol resins **16** were tagged, pooled, suspended in THF (60 ml), and gently mixed on a tabletop shaker for 1 hr followed by

mixing in DCM (60 ml) for 30 min. The resin was filtered and dried under vacuum. The dried resin (3.7 g) was split into 50 portions (75 mg, 0.6 mequiv./g avg, 0.045 mmol, 1.0 equiv.) and encoded for the subsequent reaction. To each of the 50 resin portions was added the appropriate nucleophile (0.5 mmol, 11 equiv.) followed by *i*-PrOH (0.5 ml). In the case of thiol building blocks or amine hydrochloride salts, DIPEA (0.087 ml, 0.50 mmol, 11 equiv.) was added. The vials were flushed with Ar, capped, and allowed to stand in an oven at 55°C 24 hr (except for nucleophiles **a22** and **a31** which were reacted for 36 hr). The reactions were filtered and washed with DMF (3 × 10 min), THF (3 × 10 min), and CH_2Cl_2 (3 × 10 min) to give 1,3-diol resin (**7**). Thirteen beads were individually cleaved and decoded, and the released compounds were analyzed by LCMS. Approximately 600 beads were set aside for inclusion in the final library.

Amino-1,3-Dioxane Resin (19)

After pooling, 1,3-diol resin **7** was split into six equal portions (705 mg, 0.55 mequiv./g avg, 0.39 mmol, 1.0 equiv.) and treated with Fmoc-amino dimethylacetal building blocks (4.27 mmol., 11 equiv.) in a solution of 0.05 M HCl in anhydrous 1,4-dioxane (14.3 ml) and TMSCl (1.27 ml, 10.1 mmol, 26 equiv.). After 4 hr, the reaction was quenched with anhydrous pyridine (7 ml), filtered, and washed with DMF (4 × 10 min) and THF (2 × 10 min). The resin was treated with 0.2 M pyridinium *para*-toluenesulfonate in 10% MeOH-THF (2 × 10 ml) for 2 hr. The resin was filtered and washed with DMF (4 × 10 min), THF (2 × 10 min), and CH_2Cl_2 (2 × 10 min). The pools were then encoded for the previous reaction. Fmoc quantitation of 34 individual beads (several from each pool except the *para*-aniline derived pool) provided an average loading level of 52 nmol/bead. Approximately 600 beads from each pool (except the *para*-aniline-derived pool) were set aside for inclusion in the final library. Ten beads were individually cleaved and decoded, and the released compounds were analyzed by LCMS. The remaining resin (4.3 g) was pooled, split into 22 portions, and encoded for the following reactions. The encoded resin was treated with 20% piperidine-DMF (3 × 2 ml) for 30 min and then washed with DMF (3 × 10 min) and CH_2Cl_2 (3 × 10 min) and dried under vacuum. The resin was suspended in CH_2Cl_2 (3 ml) with DIPEA (0.26 ml, 1.5 mmol) and DMAP (0.012 g, 0.1 mmol), and TESCl (0.15 ml, 0.9 mmol) was added. After 1.5 hr, the resin was washed with DMF (1 × 10 min), THF (2 × 10 min), and CH_2Cl_2 (3 × 10 min) to give amino-1,3-dioxane resin **19**.

Amide and Sulfonamide 1,3-Dioxanes (21) and (22)

(i) Reaction One. Amino-1,3-dioxane resin **19** (195 mg, 0.33 mequiv./g avg, 0.065 mmol, 1 equiv.) was incubated with acid or sulfonyl chloride (0.4 mmol, 0.2 M, 6 equiv.) in CH_2Cl_2 (2 ml) with 2,6-lutidine (70 μl, 0.6 mmol, 0.3 M, 9 equiv.). After 10 hr at room temperature (or 8 hr in the case of electrophiles **b2** and **b6**), the resin was filtered and washed with DMF (3 × 10 min), THF (3 × 10 min), and CH_2Cl_2 (3 × 10 min). Fifty-nine beads (five or eight beads per pool) were individually cleaved and decoded, and the released compounds were analyzed by LCMS.

(ii) Reaction Two. Amino-1,3-dioxane resin **19** (195 mg, 0.33 mequiv./g avg, 0.065 mmol, 1 equiv.) was incubated with acetic anhydride (**b11**, 94 μl, 1 mmol, 0.5 M, 15 equiv) in DMF (2 ml) with pyridine (80 μl, 1 mmol, 0.5 M, 15 equiv.). After 11.5 hr at room temperature, the resin was filtered and washed with DMF (3 × 10 min), THF (3 × 10 min), and CH_2Cl_2 (3 × 10 min). Five beads were individually cleaved and decoded, and the released compounds were analyzed by LCMS.

(iii) Reaction Three. To amino-1,3-dioxane resin **19** (195 mg, 0.33 mequiv./g avg, 0.065 mmol, 1 equiv.) was added a solution of 6-acetamidohexanoic acid (**b16**, 346 μl, 2 mmol, 1.0 M, 31 equiv.) with PyBOP (986 mg, 1.9 mmol, 0.95 M, 29 equiv.), DIPEA (435 μl, 2.5 mmol, 1.25 M, 38 equiv.) in 2:1 DMF: CH_2Cl_2 (2 ml). After 12 hr at room temperature, the resin was filtered and washed with DMF (3 × 10 min), THF (3 × 10 min), and CH_2Cl_2 (3 × 10 min). Five beads were individually cleaved and decoded, and the released compounds were analyzed by LCMS.

Carboxyamide 1,3-Dioxanes (23)

Amino-1,3-dioxane resin **19** (195 mg, 0.33 mequiv./g avg, 0.065 mmol, 1 equiv.) was incubated with anhydride (1 mmol, 0.5 M, 15 equiv.) in DMF (2 ml) and pyridine (80 μl, 1 mmol, 0.5 M, 15 equiv.). After 11.5 hr at room temperature, the resin was filtered and washed with DMF (3 × 10 min), THF (3 × 10 min), and CH_2Cl_2 (3 × 10 min). Five beads from each pool were individually cleaved and decoded, and the released compounds were analyzed by LCMS.

Imide 1,3-Dioxanes (24)

Amino-1,3-dioxane resin **19** (195 mg, 0.33 mequiv./g avg, 0.065 mmol, 1 equiv.) was incubated with anhydride (2 mmol, 1.0 M, 31 equiv.) in toluene (2 ml). After 12 hr at 110°C, the resin was filtered and washed with DMF (3 × 10 min), THF (3 × 10 min), and CH_2Cl_2 (3 × 10 min). Five or eight beads from each pool were individually cleaved and decoded, and the released compounds were analyzed by LCMS.

Urea 1,3-dioxanes (25)

Amino-1,3-dioxane resin **19** (195 mg, 0.33 mequiv./g avg, 0.065 mmol, 1 equiv.) was incubated with isocyanate (2 mmol, 2.0 M, 31 equiv.) in CH_2Cl_2. After 18 hr at room temperature, the resin was filtered and washed with DMF (3 × 10 min), THF (3 × 10 min), and CH_2Cl_2 (3 × 10 min). Five or eight beads from each pool were individually cleaved and decoded, and the released compounds were analyzed by LCMS.

Parallel Synthesis of Amine and Diol Sublibraries

Resins loaded with epoxy alcohols **2** and **4** (6–8 mg) were placed in 4 ml vials to which were added isopropanol (300 μl), nucleophile (0.3 mmol), and, for thiols and amine hydrochloride salts, DIPEA (52 μl). The vials were flushed with argon, sealed with teflon-lined caps, and allowed to react for 24 hr at 55°C (except for nucleophiles **a22** and **a31** which were reacted for 36 hr). Resin was filtered, washed with DMF (3 × 10 min), THF (3 × 10 min), and CH_2Cl_2 (3 × 10 min), and then dried under high vacuum. Twenty beads were individually cleaved and analyzed by LCMS. Ninety-six 1,3-diol resins were chosen for 1,3-dioxane formation and arrayed (eight beads/well) as depicted. Hydroxyl-containing nucleophiles were arrayed along the top two rows of the 96-well plate to facilitate PPTS removal of mixed acetals. Dimethylacetals (**6**, **8–11**) were dissolved in CH_2Cl_2 (0.3 M), and 50 μl of dimethylacetal solution was added to each well. This was allowed to evaporate and then dried under high vacuum in a dessicator overnight (with a capmat loosely positioned over the 96-well plate). After purging the dessicator with argon, the plate was quickly sealed with the capmat under an argon blanket. Anhydrous 1,4-dioxane (50 μl) containing 5% TMSCl and 0.2 M HCl was injected into each reaction well under argon via 25 gauge needle. After 4 hr, the reactions were quenched with pyridine (50 μl), aspirated via geltip pipette, and washed with DMF (3 × 10 min), THF (3 × 10 min), and CH_2Cl_2 (3 × 10 min). Reactions in rows A and B were also washed with 50 μl/well PPTS (0.2 M in 10% MeOH/THF), 2 × 50 min, followed by DMF (3 × 10 min), THF (3 × 10 min), and CH_2Cl_2 (3 × 10 min).

Formatting of the Parallel Library for Biological Evaluation

(i) Formatting for Fmoc Cleavage and Forward Chemical Genetic Screens. One set of amino-1,3-dioxane beads were arrayed into 96-well plates (Costar polypropylene) and subjected to 20% piperidine/DMF (100 μl/well) for 30 min under seal (Costar 6569 Thermowell Sealing Tape) to minimize evaporation. A portion of the solution (15 μl) from each well was then added to the corresponding well (already containing 285 μl of 50:45 H_2O:DMF solution) in a clear 96-well plate designed for UV absorption measurement (Costar 3635). Plates were then analyzed in a SpectraMax Plus 384 UV plate reader for absorption at 290 nm ($\epsilon = 5090$ as determined by standards tested in 96-well format) using a reference cuvette containing 1:1 H_2O:DMF with background correction from control wells. After Fmoc quantitation, the remaining beads were washed with DMF (3 × 10 min), THF (3 × 10 min), and CH_2Cl_2 (3 × 10 min), and then arrayed into 384-well plates along with 1,3-diol resin for compound release using the individual bead cleavage protocol.

(ii) Formatting for Small-Molecule Microarray Printing. Fmoc-protected amino-1,3-dioxane resin and 1,3-diol resin were arrayed in 384-well format (see Supplemental Data). After compounds were released using the individual bead cleavage protocol and separated from the beads, each compound-containing well was dissolved in DMF (24 μl) and 5 μl of this transferred to the corresponding well for the low-concentration copy of the library. After removal of DMF, all wells were dissolved in DMF (9.5 μl) to give a 5 and 1.3 mM copy of the library (assuming approximately 60 nmol/bead average loading level as determined by Fmoc quantitation) for printing.

Slide Preparation for Small-Molecule Microarrays

γ-aminopropyl functionalized glass slides (Corning) were incubated with 10 mM 8-(Fmoc-amino)-3,6-dioxaoctanoic acid, 10 mM PyBOP, and 20 mM DIPEA in DMF for 12 hr at room temperature. After extensive washing in DMF, slides were rinsed with MeOH, spun at 900 rpm for 3 min, and then dried under vacuum before further derivitization. Immediately before printing, slides were subjected to 20% piperidine/DMF for at least 45 min, washed with DMF (5 × 3 min), and then immersed into hexamethylene diisocyanate (neat). After incubating the slides for at least 10 min, excess hexamethylene diisocyanate was removed with DMF (1 × 3 min) and THF (3 × 3 min) followed by drying under a nitrogen stream before printing.

Typical Microarray Screening Protocol

Amino-1,3-dioxanes printed on slides were deprotected in 20% piperidine/DMF (45 min, room temperature), washed with DMF (4 × 3 min) and MeOH (2 × 3 min), dried, and then blocked with 3% bovine serum albumin (BSA) in pH 7.4 phosphate-buffered saline with 0.1% Tween (PBST/0.1%) over 1 hr at room temperature on a tabletop rotator. After briefly rinsing in PBST/0.1%, the slides were incubated with either unlabeled protein or fluorescently-labeled protein in PBST/0.1% with 1% BSA for 1 hr at 4°C. For labeled proteins, the slides were then washed in PBST/0.1% (3 × 5 min), ddH_2O (brief), and dried by centrifuge (1000 rpm) before scanning. For unlabeled proteins, slides were briefly washed in PBST/0.1% and then incubated with fluorescently labeled antibodies in PBST/0.1% 1% BSA for 1 hr at 4°C. Slides were then washed in PBST/0.1% (3 × 5 min), ddH_2O (brief), and dried by centrifuge (1000 rpm) before scanning. Fluorescent signals were detected with a Genepix 4000B microarray scanner (Axon Instruments).

Surface Plasmon Resonance for Determining Calmodulin Binding Constant of (42)

(i) Surface Preparation and Protein Capture. A CM5 sensor chip (Biacore BR-1000-114) was derivitized using the anti-GST capture kit protocol (Biacore BR-1002-23) as per manufacturer's instructions. The control flow cell was injected with GST (1.5 μl of a 0.2 mg/ml solution in 58.5 μl HBS-P) and the active flow cell injected with GST-CaM (0.005 mg/ml in HBS-P) for 2.5 min with a 20 μl/min flow rate.

(ii) Small-Molecule Binding Affinity Studies. Flow cell buffer was equilibrated to 5.0% DMSO in PBST/0.1% (previously filtered and degassed under 20 mm Hg vacuum for 1 hr). For the DMSO calibration curve, DMSO solutions of various concentrations (typically 3.0%–6.0% DMSO) were prepared using the same PBST/0.1% stock that was used to prepare the 5.0% DMSO running buffer. A 20 mM DMSO stock solution of compound **42** was diluted to various working concentrations and then added slowly to PBST/0.1% buffer (which had been prewarmed at 60°C for 1 min) to a final DMSO concentration of 5.0%. The compound solutions and DMSO standards were then injected into active and control flow cells and the change in refractive index monitored. The difference in refractive index change between the control and active cells due to slight variations in DMSO concentration were corrected using the DMSO calibration curve. Final response values were then obtained by standardizing response data to the response detected for blank injections (for an SPR data analysis example, see Supplemental Data).

Zebrafish Whole Organism Developmental Assays

Assay Protocol

Zebrafish assays were performed essentially as described previously [18], with compounds transferred first to assay buffer (50 μl) by pin transfer (2 × 100 nl transfer) and then this solution added to buffer containing embryos (200 μl) at the 128–256 cell stage.

Supplemental Data

The following Supplemental Data can be found at http://www.chembiol.com/cgi/content/full/11/9/1279/DC1: general protocols for molecular encoding/decoding, resin cleavage, and LCMS analysis; electrophile screening and optimization studies; library encoding tag assignments; extensive list of library quality control data; parallel synthesis model studies; small-molecule microarray spatial format; surface plasmon resonance data analysis; methyl epoxy alcohol synthetic procedures; characterization data for resynthesized compounds; structures of resynthesized compounds used in yield analysis; and purity analysis by acylation reaction class.

Acknowledgments

We are grateful to Xiaohua Li and Abram Calderon for library formatting, Jennifer Raggio and Leticia Castro for postformat bead decoding and LCMS work, Seung-Bum Park and Angela Koehler for assistance with small-molecule microarray printing and SPR analysis, and Paul Clemons for assistance with molecular descriptor calculations. S.L.S. is an Investigator at the Howard Hughes Medical Institute. We thank the National Institute for General Medical Sciences for support of this research; the National Cancer Institute (NCI), Merck KGaA, Merck & Co., and the Keck Foundation for support of the Broad Institute Chemical Biology Program (BCB, formerly ICCB); and the NCI for support of the Initiative for Chemical Genetics.

Received: May 29, 2004
Revised: July 5, 2004
Accepted: July 8, 2004
Published: September 17, 2004

References

1. Mitchison, T.J. (1994). Towards a pharmacological genetics. Chem. Biol. *1*, 3–6.
2. Schreiber, S.L. (1998). Chemical genetics resulting from a passion for synthetic organic chemistry. Bioorg. Med. Chem. *6*, 1127–1152.
3. Shogren-Knaak, M.A., Alaimo, P.J., and Shokat, K.M. (2001). Recent advances in chemical approaches to the study of biological systems. Annu. Rev. Cell Dev. Biol. *17*, 405–433.
4. Desai, A., and Mitchison, T.J. (1997). Microtubule polymerization dynamics. Annu. Rev. Cell Dev. Biol. *13*, 83–117.
5. Dammermann, A., Desai, A., and Oegema, K. (2003). The minus end in sight. Curr. Biol. *13*, R614–R624.
6. Hardwick, J.S., Kuruvilla, F.G., Tong, J.K., Shamji, A.F., and Schreiber, S.L. (1999). Rapamycin-modulated transcription defines the subset of nutrient-sensitive signaling pathways directly controlled by the Tor proteins. Proc. Natl. Acad. Sci. USA *96*, 14866–14870.
7. Kuruvilla, F.G., Shamji, A.F., and Schreiber, S.L. (2001). Carbon- and nitrogen-quality signaling to translation are mediated by distinct GATA-type transcription factors. Proc. Natl. Acad. Sci. USA *98*, 7283–7288.
8. Bernstein, B.E., Tong, J.K., and Schreiber, S.L. (2000). Genome-wide studies of histone deacetylase function in yeast. Proc. Natl. Acad. Sci. USA *97*, 13708–13713.
9. Luo, J., Su, F., Chen, D., Shiloh, A., and Gu, W. (2000). Deacetylation of p53 modulates its effect on cell growth and apoptosis. Nature *408*, 377–381.
10. Taunton, J., Hassig, C.A., and Schreiber, S.L. (1996). A mammalian histone deacetylase related to the yeast transcriptional regulator Rpd3p. Science *272*, 408–411.
11. Schreiber, S.L. (2000). Target-oriented and diversity-oriented organic synthesis in drug discovery. Science *287*, 1964–1969.
12. Sternson, S.M., Louca, J.B., Wong, J.C., and Schreiber, S.L. (2001). Split-pool synthesis of 1,3-dioxanes leading to arrayed stock solutions of single compounds sufficient for multiple phenotypic and protein-binding assays. J. Am. Chem. Soc. *123*, 1740–1747.
13. Kuruvilla, F.G., Shamji, A.F., Sternson, S.M., Hergenrother, P.J., and Schreiber, S.L. (2002). Dissecting glucose signaling with diversity-oriented synthesis and small-molecule microarrays. Nature *416*, 653–657.
14. Blackwell, H.E., Pérez, L., Stavenger, R.A., Tallarico, J.A., Eatough, E.C., Foley, M.A., and Schreiber, S.L. (2001). A one-bead, one-stock solution approach to chemical genetics: part 1. Chem. Biol. *8*, 1167–1182.
15. Burgess, K., Liaw, A.I., and Wang, N. (1994). Combinatorial technologies involving reiterative division/coupling/recombination: statistical considerations. J. Med. Chem. *37*, 2985–2987.
16. Clemons, P.A., Koehler, A.N., Wagner, B.K., Sprigings, T.G.,

Spring, D.R., King, R.W., and Schreiber, S.L. (2001). A one-bead one-stock solution approach to chemical genetics: part 2. Chem. Biol. *8*, 1183–1195.

17. MacBeath, G., Koehler, A.N., and Schreiber, S.L. (1999). Printing small molecules as microarrays and detecting protein-ligand interactions *en masse*. J. Am. Chem. Soc. *121*, 7967–7968.
18. Peterson, R.T., Link, B.A., Dowling, J.E., and Schreiber, S.L. (2000). Small molecule developmental screens reveal the logic and timing of vertebrate development. Proc. Natl. Acad. Sci. USA *97*, 12965–12969.
19. Stainier, D.Y., Fouquet, B., Chen, J.N., Warren, K.S., Weinstein, B.M., Meiler, S.E., Mohideen, M.A., Neuhauss, S.C., Solnica-Krezel, L., Schier, A.F., et al. (1996). Mutations affecting the formation and function of the cardiovascular system in the zebrafish embryo. Development *123*, 285–292.
20. Milan, D.J., Peterson, T.A., Ruskin, J.N., Peterson, R.T., and MacRae, C.A. (2003). Drugs that induce repolarization abnormalities cause bradycardia in zebrafish. Circulation *107*, 1355–1358.
21. Langheinrich, U., Vacun, G., and Wagner, T. (2003). Zebrafish embryos express an orthologue of HERG and are sensitive toward a range of QT-prolonging drugs inducing severe arrhythmia. Toxicol. Appl. Pharmacol. *193*, 370–382.
22. Haggarty, S.J., Koeller, K.M., Wong, J.C., Butcher, R.A., and Schreiber, S.L. (2003). Multidimensional chemical genetic analysis of a combinatorial library of deacetylase inhibitors using cell-based assays. Chem. Biol. *10*, 383–396.
23. Sternson, S.M., Wong, J.C., Grozinger, C.M., and Schreiber, S.L. (2001). Synthesis of 7200 small molecules based on a substructural analysis of the histone deacetylase inhibitors trichostatin and trapoxin. Org. Lett. *3*, 4239–4242.